

Influence of Particulate Transport on Filtration Experiments in a Vertical Filter Vessel

Jurgen B. Roman,* Antoine J.B. Kemperman, Walter G.J. van der Meer, and Jeffery A. Wood*

Cite This: <https://doi.org/10.1021/acs.iecr.4c04519>

Read Online

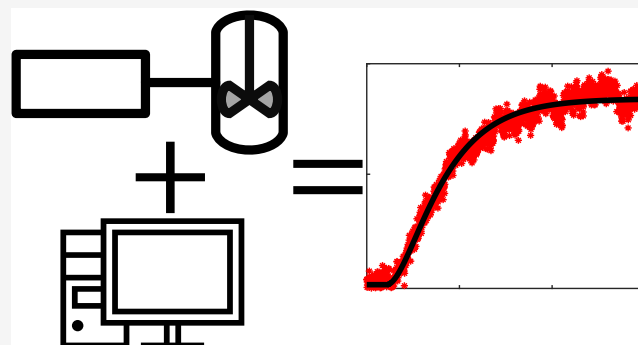
ACCESS |

Metrics & More

Article Recommendations

Supporting Information

ABSTRACT: Solid–liquid filtration is a versatile unit operation widely used within industry. In this work, we determined the residence time distribution of fluids and particles in a vertical filter vessel in order to describe the complete behavior of cake filtration experiments. By combining the residence time distribution with a lag time due to transport along the length of the filter element, we were able to describe the whole filtration step using nonlinear parameter estimation of two parameters. Analyzing the difference between the cake filtration-only model and experiments can help inform us about when other particle retention mechanisms are occurring. Our presented approach can help avoid the need for arbitrary cropping and linearization of data when analyzing cake filtration experiments. Furthermore, it is of value for describing and controlling dynamic cake filtration operations.



INTRODUCTION

For the separation of solids from fluids, filtration is a widely applied technology in the food, chemical, ceramic, and mineral processing industries.¹ For these applications, a wide variety of filtration systems have been developed in the past century.² One of the most common methods of solid–liquid separation is cake filtration, where the solids are deposited on a porous filter element (often referred to as a filter cloth) while liquid can pass through the pores. This in turn leads to a buildup of a porous solid layer on top of the filter element, increasing the hydraulic resistance over time.

Cake filtration has been studied since the earliest days of the chemical engineering discipline.³ Ruth et al. (1933, 1935) published a very informative series of papers analyzing early work and laying the groundwork for the analysis of constant pressure experiments.^{4–7} Although the application of cake filtration is still widespread in industry, the amount of academic research into this topic dwindled in the second half of the last century. Even though the popularity of the subject has subsided in academia, research into this crucial separation process continues in both a fundamental and more applied setting.^{8–10}

Analysis of solid–liquid separation experiments is often done according to the “laws of filtration” first coined by Hermans and Bredée (1935),¹¹ which build upon the work of Ruth et al. (1933) regarding the analysis of constant pressure experiments.⁴ This approach is based on transforming numerical derivatives of the obtained data in four ways, each corresponding to a different filtration mechanism:

$$\frac{d^2t}{dV^2} = k_1 \left(\frac{dt}{dV} \right)^{k_2} \quad (1)$$

Depending on the mode of filtration, the exponent k_2 should take a specific value: 0 for cake filtration, 1 for intermediate blocking, 1.5 for standard blocking, and 2 for complete blocking.¹¹ Each of these filtration modes corresponds to a specific method by which the solids are deposited on or in the filter cloth. Although this analysis has endured until the modern day, its ability to actually identify particle retention mechanisms has been questioned recently.¹² Tien and Ramarao bring up that assumptions on which the analysis is based are often incorrect or at best approximate and the distinction between filtration modes like intermediate and complete blocking is arbitrary at best.¹² Furthermore, multiple particle retention mechanisms can occur simultaneously, for which this method does not provide a solution.¹ Lastly, values for these equations are often determined by linearization and cropping of the data, which skews results and introduces bias into the analysis.¹⁴

Compared with the linearization of the experimental data, a more robust method is nonlinear parameter estimation. The

Received: November 28, 2024

Revised: February 7, 2025

Accepted: February 11, 2025

earliest, as far as we are aware, although still quite recent, application of this method for cake filtration is in the fouling of microfiltration membranes.¹⁵ Recently, multiple authors have shown the advantages of using nonlinear parameter estimation methods for cake filtration experiments.^{14,16} By avoiding the bias introduced by the data linearization and cropping, more accurate information on the formed cakes can be gathered, possibly alleviating some of the difficulties encountered in filtration equipment scale-up.¹⁷

In the most general sense, the process of cake formation, where particles are deposited on top of similar particles, is a simple case of fluid flow through a porous medium. This can, in turn, be described by using Darcy's law, where ΔP is the pressure difference in Pa, η is the viscosity of the liquid in Pas, R is the medium resistance in m, ϕ_V is the volumetric flow rate in m³/s and A is the surface area in m²:

$$\Delta P = \eta \phi_V \frac{R}{A} \quad (2)$$

Here, the resistance is comprised of resistance of the bare filter medium, the cake layer itself, and possible interactions between the medium and solids like filter blinding. If one knows the amount of solids that deposited on the filter cloth at each moment in time:

$$\Delta P = \eta \phi_V \frac{R_{\text{cake}} + R_0}{A} \quad (3)$$

$$\text{where: } R_{\text{cake}} = \int_0^{t_{\text{end}}} \alpha C(t) \phi_V dt \quad (4)$$

where R_0 is the initial resistance of the filter element and the clear cloth, R_{cake} is the cumulative cake resistance, α is the specific resistance of the cake in m/g and $C(t)$ is the concentration of solids hitting the filter cloth/the built up cake at time t .

Another often discussed, but rarely quantified, phenomenon in filtration studies is the transport of the particulates inside the filtration vessel during filtration. Previous research has found the influence of particulates on fluid behavior in stirred vessels and pipe flow.^{18–20} Furthermore, in data analysis, the initial parts of filtration are often neglected because the system is “not yet in steady state,”

while this period could contain crucial cloth-particle interaction information. Recently Benz et al. showed that selecting more appropriate laboratory equipment can substantially reduce the amount of data that needs to be left out,²¹ but this does not eliminate the arbitrary selection of data. The selection of data from experimental filtration data was also discussed by Thomas Buchwald,¹⁶ using the residuals of a nonlinear regression in order to select the portion of data that exhibits cake filtration behavior.

Classically used laboratory equipment like compression permeability cells are known to introduce artifacts due to wall friction, causing nonhomogeneous structures and time lag.²² In order to generate information that is more accurate for industrial-scale cake filtration operations, laboratory filter systems and operations should closely represent the final application. This however means that some of the simplicities of conventional laboratory equipment, like a constant slurry concentration, have to be sacrificed. By identifying the residence time distribution (mixing behavior) of the filtration vessel, it should be possible to account for this such that the whole filtration step can be described. Since the particulate

transport is determined separately from the filtration, no additional fitting parameters were required for describing the actual filtration experiment, avoiding the possibility of attributing filtration phenomena to transport phenomena. This allows for using equipment that is more similar to that used in an industrial setting and can avoid the need to crop data arbitrarily in order to describe the experimental results.

In this work, we study the separation of solids from liquids using a vertical filter element, akin to a classical candle filter. The goal is to investigate the cake formation process using a combination of residence time distribution models and nonlinear parameter estimation. By investigating different possible situations (different impermeable locations on the filter cloth, precoat filtration, and multiple particle filtration) and using a set of simple measurements, we elucidate how particulate transport affects the cake filtration process in order to describe the whole filtration step.

METHODOLOGY

Cake filtration experiments were performed on a “Cricketfilter” element inside of a vessel, both provided by Amafilter, Filtration Group BV (Lochem, The Netherlands). The filter element is called a “Cricketfilter,” due to its shape being similar to a cricket bat. A simplified schematic representation of the experimental setup can be seen in Figure 1. Pictures of the

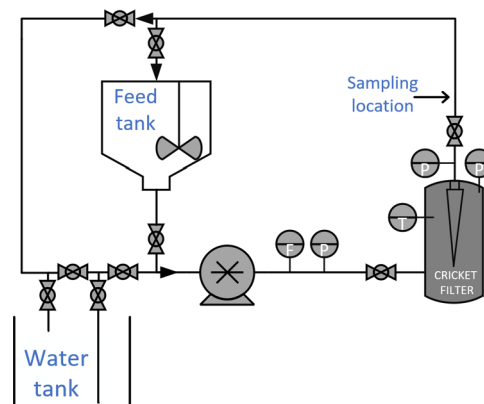


Figure 1. Schematic representation of the cake filtration setup.

filter element alongside the filter cloths used can be found in Figure S1. The liquid/slurry enters the tank and then impacts a distributor to spread it out over the tank volume; this can also be seen in the two-dimensional sketch of the filter vessel in Figure S21. Pumping was performed either with a gear pump (experiments performed at 2 or 2.8 L/min) or with a progressive cavity pump (experiments performed at 3 L/min).

The experiments were performed by setting a constant flow rate using feedback from the flow meter to the pump. Initially, the system was pressurized by flowing demineralized water with KCl (at a conductivity of approximately 200 $\mu\text{S}/\text{cm}$, required for the flow meter) through the system. The solids were then mixed with a solution of the same KCl concentration in the feed tank by a combination of stirring and intermittent gas-sparging from the feed tank outlet (only during mixing before the experiment) to counteract sedimentation inside the conical outlet. The feed tank is equipped with a downward-pumping impeller to create as much axial mixing as possible, keeping the solids evenly suspended.

The filtration experiment was started by simultaneously closing both valves connected to the water tank and opening both valves at the inlet and outlet of the feed tank to recirculate the liquid over the feed tank instead of the water tank. This approach ensures that the system is pressurized before the filtration starts, and any measured difference in pressure can be attributed to the filtration of the solids right from the start of the experiment. Recirculating the liquid back to the feed tank ensured that all added particles would be fed to the filter vessel, and any initial breakthrough of the filter would also end up in the feed again. While the solids remained well suspended in the feed tank, it was not possible to completely prevent sedimentation inside of the filter vessel, leading to the “loss” of some particles (up to a maximum ≈ 15 mass%). Most of the particles that sedimented inside the filter tank were larger particles; see Figure S5 in the Supporting Information. No evidence was found that the sedimentation was severe enough to alter the particle size distribution between the inlet and outlet of the filter tank. Therefore, it was assumed that the influence of the sedimentation was minor.

During filtration, the feed flow, temperature inside the filter vessel, and pressure drop over the filter element (by deducting the pressure at the outlet from the pressure inside the filter vessel) were recorded every second by averaging the data acquired since the previously recorded value. The feed flow was recorded using a magnetic inductive flow meter (Mass Flow online, MVM-030-PA), the temperature was measured using a PT1000 RTD sensor (RS Pro, 334-2616) and pressures were measured via probes (RS Pro, 828-5741). The conductivity of the solution at the outlet of the filter vessel was measured for some experiments (Icon Process Controls Ltd., ProCon C450). All of these sensor elements were connected to a Labview program, which also allowed control of the speed of the pump via a PI controller to keep the filtration rate constant. The filtration was operated until the pressure over the filter element became stable, meaning there were no more solids in the feed tank. After this, the resulting cake layer was dried by flowing N_2 for approximately half an hour, and the dried cake layer was inspected.

In order to estimate the residence time distribution of the filter vessel, the water tank and feed tank were filled with solutions varying in KCl concentration (i.e., differing in conductivity). By switching from one vessel to the other and not recirculating the outlet, we could perform a step-change experiment could be performed. The transient response of the change in conductivity from the initial feed conductivity to the new feed conductivity was used to describe the residence time distribution of the vessel. In a similar manner, the residence time distribution of solids was determined by taking samples at the outlet of the filter (without a filter cloth) and looking at the liquid/sediment ratio after letting the samples settle.

Particle sizes were determined by dynamic light scattering using a Malvern mastersizer 2000 with a hydro 2000s (A) module. For cellulose fibers, the sizes given by the manufacturer have been stated.

MATERIALS

The filter element consists of a metal support structure with an outlet tube in the middle and large holes (4.9 mm) along the outside. Over this metal frame, a very coarse and sturdy polypropylene cloth was applied to prevent the overlaying filter cloth from getting “pulled” into the metal support holes. Finally, the finer cloth is placed on top and fixed on the metal

support using an Oetiker O-clip. Pictures of the filter element and the overlaid cloths are provided in the Supporting Information (Figure S1).

Filtration cloths with a size rating of $200 \mu\text{m}$ made from nylon were used (Lampe Technical Textiles BV, Sneek, The Netherlands). All cloths were made from sheets that were cut and welded into a tubular shape, leaving one side of the cloth to have an impermeable strip. The bottom of the cloths was joined and heat melded together. Afterward, a layer of epoxy glue was applied to shut them completely.

The materials used for filtration were (ligno)cellulose fibers/particles of different sizes (obtained from J. Rettenmaier & Söhne GmbH + Co KG) and pulverized activated carbon particles (Norit, type “CASP F”). An overview of particle sizes is given in Table 1, and full particle size distributions can be found in the Supporting Information.

Table 1. Approximate Sizes of Used Particles Measured Using Dynamic Light Scattering^a

particle name	size (d10%, d50%, d90%)
lignocellulose type NF400	11, 65, 246 μm
lignocellulose type NF900	18, 93, 338 μm
pulverizes activated carbon type CASP-F	5.4, 19, 43 μm
	size ($W \times L$)
cellulose type BWW-40	$20 \times 200 \mu\text{m}$

^aValues for cellulose fibers type BWW-40 were provided by the manufacturer.

RESULTS

Filtration Results. A representative pressure versus time curve during filtration can be seen in Figure 2. The initial

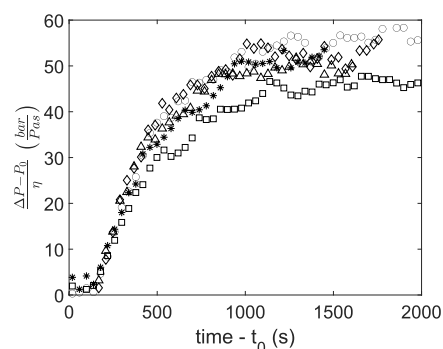


Figure 2. Data from 5 repeat experiments of NF400 lignocellulose particle filtration on a $200 \mu\text{m}$ rated cloth. Each different symbol represents an individual experiment. Every 40 data points were averaged for clarity. Flow rate was 2.8 L/min , and the slurry contained 225 g of lignocellulose particles.

pressure drop, measured with only water flowing over the element, was subtracted in order to account for the resistance of the setup and cloth. In general, the differences between the experiments were minor (see Supplementary Figures S3 and S4). Furthermore, each curve was shifted to the left depending on the time “ t_0 ” when the feed was switched from pure water to slurry. This time was chosen when the initial pressure drop “ P_0 ” attained a stable value. From Figure 2, it can be seen that repeat experiments show the same behavior over time. Only 1 out of 5 experiments shows slightly deviating behavior (a lower pressure drop, square symbols). It could be that slightly more

sedimentation took place during this experiment or an operating error was made.

In order to verify that we were measuring the pressure drop due to cake filtration, the linearity of the pressure increase with added mass was checked by filtering increasing amounts of mass, which were added in intervals to the feed tank, as can be seen in Figure 3. The behavior is linear, indicating cake

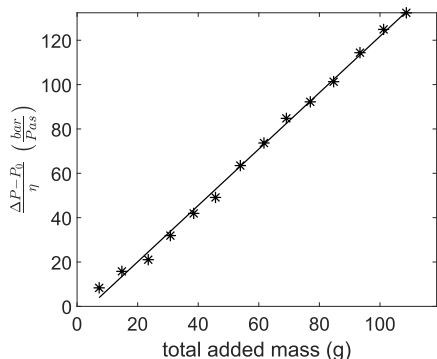


Figure 3. Data from an experiment of NF900 lignocellulose particle filtration on a 200 μm rated cloth. Mass was continuously added in intervals, and then a steady pressure drop was recorded after some time (about 15 min). Flow rate was 2 L/min and around 7 g of particles were added each time.

filtration behavior and no substantial influence of other filtration modes (standard blocking, complete blocking, or intermediate blocking) or compressibility of the cake when using lignocellulosic particles.

Residence Time Distribution. From Figure 2, we can see that there is a substantial lag time (approximately 170 s) between the start of the experiment and the increase in pressure drop over the filter element. In order to check how much of this lag time was caused by transport toward the filter surface, residence time distribution experiments were performed. Figure 4 shows the cumulative distribution function for both solids (cellulose fibers) and dissolved salt in a step change experiment. The cumulative distribution function is defined as follows:

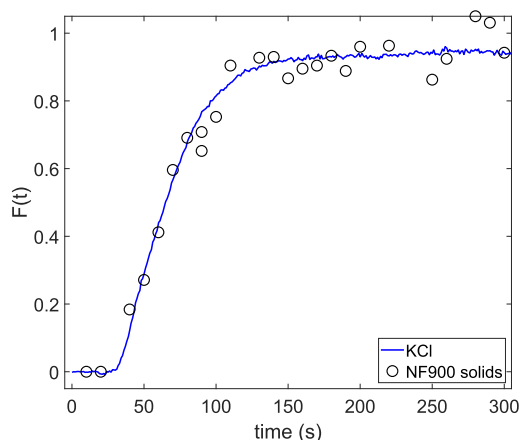


Figure 4. Cumulative distribution function (t) of step change experiments using both lignocellulose particles (NF900) as solids and KCl as a dissolved tracer. Flow rate used was 3 L/min with 30 g/L of solids.

$$F(t) = \left(\frac{C_{\text{outlet}}}{C_{\text{inlet}}} \right) \quad (5)$$

The solid concentration was determined by letting the outlet samples settle and determining the ratio of the height of the sediment to the height of the liquid. For KCl the conductivity of the outlet samples was measured and used as an analogue for the concentration. In these experiments, we stayed in a linear conductivity vs KCl concentration regime (<10 mM KCl).

From Figure 4, it can be seen that the dissolved tracer (KCl) is a good indicator of the residence time distribution of the solid particulates in the applied flow regime (

$$Re = \frac{\rho v d}{\eta} \approx \frac{998 \times 5.7 \times 10^{-4} \times 0.168}{10^{-3}} = 95,$$

$$Pe = \frac{vL}{D} \approx \frac{5.7 \times 10^{-4} \times 0.3}{10^{-9}} = 2.6 \times 10^5$$

inside of the tank, when ignoring entrance effects, such as the liquid distributor behind the inlet of the tank. Due to the high similarity, the more reliable conductivity data was used in order to fit residence time distribution models. The influence of segregation of particles was also investigated by measuring the particle size distributions for every sample in Figure 4 and in the feed tank, which are given in the Supporting Information in Figures S3–S5. No segregation of particle sizes over time or in the feed tank was observed, leading us to assume a constant homogeneous suspension in this case. It could very well be that other particle systems (especially particles of higher density) would show a measurable segregation effect.

In order to use residence time distributions, it is customary to model the system as a combination of idealized mixing elements.²³ These elements generally include the plug flow reactor (PFR, no axial mixing) and the ideally continuously stirred tank reactor (CSTR, perfect axial mixing). From our F-curves, we can deduce that we need a PFR to describe the initial delay and one or more CSTRs to describe the curvature. We allow for the CSTRs to have different representative volumes since this could represent different internal regions inside the filter vessel. The following F-functions were derived for a PFR in series with a single CSTR or 2 CSTRs of unequal volume in series:

Single CSTR with a PFR:

$$F(t) = 1 - e^{-(t-\tau_d/\tau_1)} \quad (6)$$

Two CSTRs in series with a PFR:

$$F(t) = 1 - \frac{\tau_1}{(\tau_1 - \tau_2)} e^{-(t-\tau_d/\tau_1)} - \frac{\tau_2}{(\tau_2 - \tau_1)} e^{-(t-\tau_d/\tau_2)} \quad (7)$$

Here t is time, τ_d is the residence time in the PFR (the delay time) and τ_1 and τ_2 are the residence times inside of the respective CSTRs.

In Figure 5, the cumulative response to a step change in conductivity in the system is shown together with the model corresponding to eq 6, fitted by using nonlinear parameter estimation. A representation of a single PFR with a single CSTR represents the system well. Adding an extra CSTR did not improve agreement, and the confidence intervals of the fitted parameters included 0, see Table 2. The normality of the residuals of the 1 CSTR model was checked visually, as shown in the Supporting Information, in Figure S9.

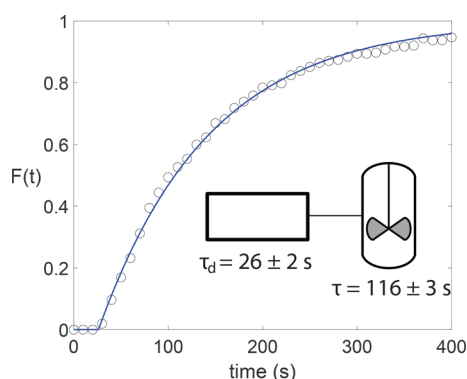


Figure 5. Cumulative distribution function $F(t)$ and fitted single CSTR + PFR model of a step change experiment with KCl as a dissolved tracer at a flow rate of 2.8 L/min.

Table 2. Residence Time Distribution Fitting Parameters and Diagnostics

model	parameters (s)	RMSE ^a
single CSTR + PFR	$\tau_d = 26 \pm 2$	1.8×10^{-4}
	$\tau_1 = 116 \pm 3$	
two CSTRs + PFR	$\tau_d = 27 \pm 1.5 \times 10^6$	1.9×10^{-4}
	$\tau_1 = 115 \pm 3$	
	$\tau_2 = 0.01 \pm 1.5 \times 10^6$	

^aResidual mean squared error.

The difference in transient response in Figures 4 and 5 is quite large, even though the difference in the applied volumetric flow rate is minor (<10%). The difference in the initial breakthrough time can be explained by the larger tubing used in the experiment shown in Figure 4, leading to a larger lag time before the breakthrough occurs. The difference in transient behavior is likely caused by the concentration of particles affecting the hydrodynamics of the system. The effect of solids concentration on residence time was also found by Fan and Fu as well as Palmieri et al., although both found an increasing residence time with increasing suspension concentration while we observed a lower mean residence time at higher solids concentration.^{18,19} A more recent study by Hogendoorn et al. showed that the concentration of particulates along with geometry influence the critical Reynolds number for the onset of turbulent flow, likely leading to the different residence time distribution behavior observed here.²⁰

The lignocellulose particle concentration of 30 g/L, corresponding to a volumetric particle concentration of 18%, is beyond what can be considered a dilute suspension with no influence on the residence time in theory. However, in our system, the concentration of the suspension, both in the feed tank and in the filtration tank, during the filtration experiments is never constant. This makes accounting for the effect of the particle concentration on the residence time distribution complicated. Therefore, we opted to use the “particle-free” residence time distribution as an initial attempt to quantify the particulate transport during filtration.

Effect of the Filter Height. In order to study the transport of solids along the height of the filter, the cloths were blocked off using duct tape, leaving identical permeable areas at different heights. We divided the permeable areas into “sections”, numbered as shown in Figure 6. Pictures of these filter cloths with corresponding “section numbers,” can be

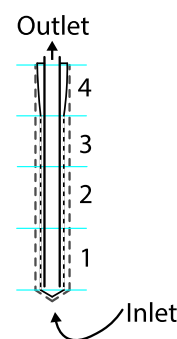


Figure 6. Locations of open sections on the cloths used.

found in the Supporting Information. Using this approach, the filtration area was constant across the tests, but the location of this area could be altered. The resulting information can give insight into the effect of the length of filter elements placed in vertical filter vessels.

From Figure 7, it can be seen that Sections 1, 2, and 3 show the same filtration behavior, but the end of the filter element

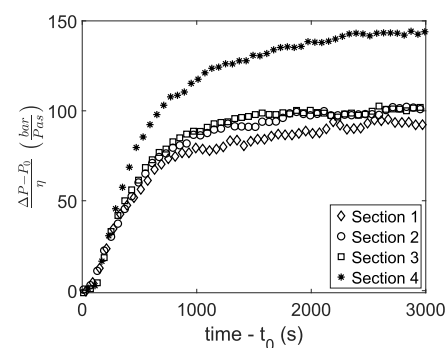


Figure 7. Effect of open cloth section on pressure drop behavior of filtration tests. Shown points are the mean of 60 recorded points. Different symbols indicate separate filtration tests on different sections, where 1–4 indicate going “up” the cloth (away from the inlet). Flow rate was 3 L/min and 40 g of lignocellulose NF900 particles were used.

(Section 4) shows a distinctly different behavior. We suspect this is either due to the metal support under this part of the cloth being impermeable or the shape of the metal support element being different in this section. However, the contribution of this part of the element in large-scale installations is only minor, since it constitutes only 3% of the total filter element area, compared to 26% of the total filter element area in our equipment. Therefore, experimental tests on smaller filter elements like this one would probably best be performed by making the filter cloth impermeable on the top section of the element.

Using these NF900 lignocellulose particles as filtration material we were not able to measure a difference in the time for the start of filtration, although we expected that Section 1 (closest to the inlet of the vessel) would show an earlier increase in pressure drop. In a different experiment with the NF400 lignocellulose particles, the same as were also used in Figure 2, we were able to observe this effect as can be seen in Figure 8. Likely the fact that the NF400 lignocellulose particles gave a higher pressure drop allowed us to show this effect using this material. There is a clear difference of 50 s between the start of filtration in Section 1 and the start of filtration in

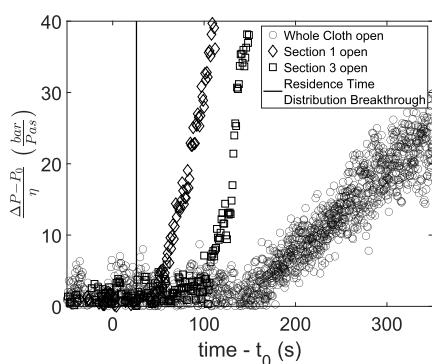


Figure 8. Effect of open cloth location on pressure drop behavior of filtration tests. Different symbols indicate separate filtration tests on different locations, where 1 to 4 indicate traveling upward on the cloth (away from the inlet). Flow rate was 2.8 L/min and 46 g of lignocellulose NF400 particles were used.

Section 3. Section 3 is located about 14 cm above Section 1, giving us a “linear velocity” of the particles inside the filter tank of $\frac{14 \text{ cm}}{50 \text{ s}} = 0.28 \text{ cm/s}$. The value is slightly higher than what one would obtain by dividing the flow rate by the area of the filter vessel, which yields 0.23 cm/s. The whole cloth has a length of 28 cm, so it would take $\approx 100 \text{ s}$ for the particles to reach the top of the filter cloth based on the linear velocity determined from Figure 8. This gets us close to the apparent starting time of the “whole cloth open” case.

Impact on Cake Filtration Modeling. In order to improve our understanding of the cake filtration process and investigate cloth-particle interactions, it is crucial to be able to model the whole filtration step. Our previous results have shown that a large part of the initial “time lag” in cake filtration can be attributed to the transport characteristics of our experimental setup. This transport can be in the form of transport toward the filter vessel, mixing inside of the filter vessel, or transport along the cloth surface. Using the results described previously, we construct a transient model describing the cake filtration process in our vessel.

For modeling the system, we use the residence time distribution model obtained from the conductivity measurements to determine the amount of solids colliding with the filter cloth in combination with Darcy’s law (eq 3) to describe the pressure drop. Equations were transformed into the Laplace domain and then subsequently solved using Matlab-Simulink (version 2022b). Since we previously already saw a large delay between the residence time distribution breakthrough and the start of filtration in Figure 8, as expected, this does not capture the transient behavior, which can be seen from the dotted line in Figure 9. Using the 100 s it takes to transport material along the filter cloth determined previously from Figure 8, we can match the start of filtration but not capture the subsequent behavior as can be seen from the dashed line in Figure 9. Both approaches can also be combined, by simply increasing the PFR residence time by the time it takes to transport particulates along the cloth length. This does allow us to describe the transient behavior of the cake filtration, but an extra delay time of 68.9 s instead of 100 s does agree better with the experimental results. Likely only the length of the “permeable” part of the metal support should be taken to calculate the delay time (see Sections 1–3 in Figure 6) since the top widened part of the support has no holes for liquid to flow through. The length of this permeable

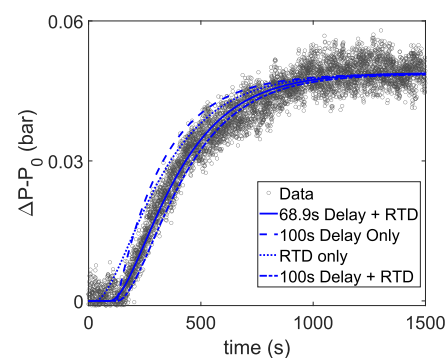


Figure 9. Filtration data are from Figure 2, excluding the one experiment that behaved differently. Lines represent a model based on Darcy’s law, accounting for transport toward the cloth by using residence time distributions measured through a KCl step change experiment and/or transport along the cloth.

part of the metal support is 20 cm, which with our determined velocity along the cloth of 0.28 cm/s would lead to a predicted delay time of 71.4 s, which is very close to the value of 68.9 s determined by nonlinear parameter estimation.

The model based on the “particle-free” residence time distribution is able to describe the experimental results well, even though it was observed in Figures 4 and 5 that the particulate concentration has a substantial influence on the residence time distribution of the liquid in the filter vessel. It is possible that on the length scale of the filtration step, the influence of the particulate concentration on the hydrodynamics in the filter vessel is only minor. Another explanation is the lower maximum particulate concentration, due to the particulate concentration in the feed tank diminishing over time.²⁰ In the filtration experiments, the particulate volume fraction in the filter tank never reaches above (on average) 6 V %, while in the step change experiment, the feed particulate volume fraction was around 18 V %. It should be noted that there could be many other situations (different filter geometry, throughput or e.g. more dense solids), where using a particle-free residence time distribution does not provide satisfying results.

In the case shown in Figure 9 both the value of the specific cake resistance α and the transport delay are used as fit parameters, and their values can be seen in Table 3. Most of

Table 3. Results of Nonlinear Parameter Estimation by Fitting the Model Accounting for Darcy’s Law, the Residence Time Distribution, and Transport Delay across the Cloth to the Experimental Data

parameter	value
specific cake resistance “ α ”	$2.75 \times 10^7 \pm 8.1 \times 10^4 \text{ m/g}$
delay across cloth	$68.9 \pm 1.3 \text{ s}$

the data is scattered nicely around the fitted line and parameter confidence intervals determined from the regression are small. The residuals are very well normally distributed and show no trend over time (shown in Supporting Information Figures S11 and S12, respectively). Furthermore, since 4 repeat experiments were performed, we did an F-test for lack-of-fit but did not find evidence of lack-of-fit. Likely using more open locations on the cloth could give us a more exact starting time, but only using 2 locations and assuming the velocity is

constant already apparently provides a very good approximation.

Aside from transport along the length of the cloth, there could be multiple other explanations for the observed behavior, the 3 most obvious explanations are possible inaccuracies of the pressure sensors used (leading to very small pressure drops not being measured), a certain threshold concentration that needs to be achieved before the slurry consolidates into a cake and breakthrough of particles through the cloth back to the feed tank. The possible inaccuracy of the pressure sensors, however, cannot explain this severe delay between the rise in pressure drop in the model and in the experiment. A threshold concentration before the formation of a cake layer starts has been mentioned before, by for example Stamatakis and Tien among others.²⁴ Initial breakthrough through filters in solid–liquid separation was recently also observed by Mukai et al., where accounting for the initial breakthrough let them describe their filtration results.¹³ Discussions of these possibilities, alongside a 2D CFD simulation to solve for the pressure drop over time of the system, are available in the [Supporting Information](#).

Multiple Particle Filtration. Previously we have looked at the transport of only a single fraction of solids, which are easily filtered on top of our cloth. However, often in solid–liquid separations, multiple solid fractions are to be separated simultaneously, leading to inhomogeneous cake structures. One of these situations is the removal of fine particles by employing filter-aid filtration, where an easy-to-filter solid (the filter-aid) is added to a slurry that is found to be difficult to separate since the fines would normally pass through the cloth unimpeded.²⁵ The filter aid is employed to reduce the resulting pressure drop over the formed cake and improve “the filterability” (removal rate) of the particles. Here we investigate the difference between using a common filter-aid material (cellulose fibers) as both a typical body-aid (filtered simultaneously with the particles) and as a precoat material (filtered separately before the particles). Pictures of cakes formed by precoat and simultaneous filtration can be seen in [Figure 10](#), although these specific filtrations will not be discussed. Since the filtration material was limited, we performed these filtrations on the cloth only open in “Section 1” (close to the inlet of the vessel). From [Figure 11](#) it can be seen that for precoat filtration the final pressure drop is consistently higher than for the simultaneous filtration experiments, using the same amount of cellulose as either the precoat or body-aid material. Next, we want to investigate if we again can see a difference in the formation time depending on the mode of filter-aid filtration employed.

In the filtration results in [Figure 12](#), two distinct groupings appear again when looking at the development of the pressure drop at the start of filtration. The earlier increasing pressure drop corresponds to the precoat filtration, and the later increase in pressure drop corresponds to the simultaneously filtered cellulose and activated carbon. Even though precoat filtration does not help with reducing the pressure drop of the cake layer, it does help the filtration take place faster. With precoat filtration on the cloth with only Section 1 open, there also seems to be very little delay between measuring a difference in the solution conductivity (mixing) and the increase in the pressure drop. The colored symbols in [Figure 12](#) give an indication of the degree of mixing of the fluid in the tank at the start of the experiment and the new feed solution containing the particles since both were given different



Figure 10. Photographs of the outside and inside of cakes formed by precoat filtration (left) or simultaneous filtration (right) of cellulose fibers and pulverized activated carbon.

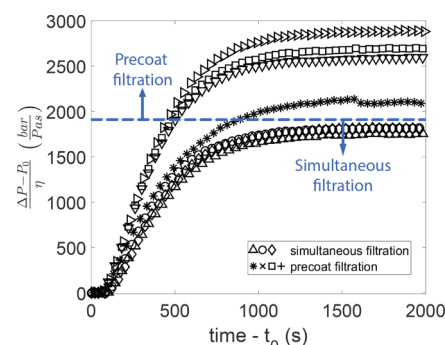


Figure 11. Difference in pressure drop behavior in simultaneous filtration vs precoat filtration of 14 g of activated carbon (CASP-F) with 6 g of cellulose (BWW-40) as the filter aid (used as the precoat or the body-aid). The flow rate is 3 L/min and a cloth only open on “location 1” was used.

conductivity. The “mixing” as indicated from 0 (unmixed) to 1 (completely mixed) was calculated as follows:

$$\text{mixing} = \frac{\sigma - \sigma_0}{\sigma_{\text{final}} - \sigma_0} \quad (8)$$

Here, σ is the conductivity of the solution measured at the outlet of the filtration vessel in $\mu\text{S}/\text{cm}$, σ_0 is the conductivity as measured before filtration is started and σ_{final} is the conductivity as measured at the end of the filtration. For the mixing behavior of the liquid as determined from these conductivity measurements in [Figure 12](#), we see the measurement for simultaneous filtration grouped up, away from the data when doing precoat filtration. The simultaneous filtration shows a more rapid rise toward the new outlet conductivity

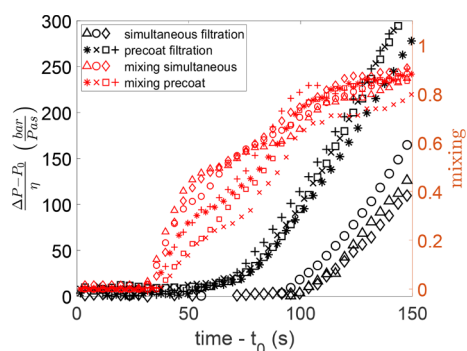


Figure 12. Filtration behavior at start of filtration including the breakthrough of the fluid as measured by a difference in conductivity before starting filtration and during filtration.

(the mixing parameter increases faster), indicating a distinctly different behavior. It is likely that the difference in mixing behavior is caused by the difference in particulate concentration.²⁰ Although there is a distinct difference in behavior, it is only slight, and the onset time of liquid breakthrough is not affected.

We compare our model to the pressure drop data from one of the precoat filtrations shown in Figure 11. When doing precoat filtration of activated carbon on cellulose using a cloth only open on location 1 (closest to the inlet), we observed very little lag time between a conductivity change and the pressure drop increasing, meaning our model should be more accurate without needing extra fitting parameters. In Figure 13 the

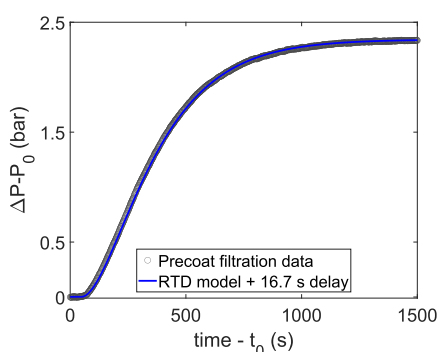


Figure 13. Filtration data from Figure 11 for precoat filtration, fitted with the residence time distribution model and accounting for transport across the filter cloth (where only “location 1” is open in this experiment).

resulting fit of the model to the precoat data is shown, accounting for the residence time distribution determined for this setup and transport across the 5 cm of open cloth length (adjusted for different flow rates used):

$$\text{Delay time} = \frac{5 \text{ cm}}{0.28 \text{ cm/s}} \frac{2.8 \text{ L/min}}{3 \text{ L/min}} = 16.7 \text{ s} \quad (9)$$

Previously, we fitted both a value for the specific cake resistance and the extra delay time due to transport along the cloth. By accounting for the transport phenomena, the only fitting parameter left in this case is the specific cake resistance value α , which here comes to a value of $4.83 \times 10^9 \pm 1.8 \times 10^6$ m/g. The fit of the model to the precoat data in Figure 13 might seem in good agreement at first glance; however, after inspection of the residuals (Figure 14) it quickly becomes

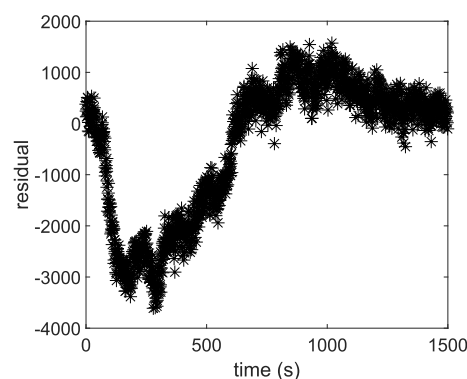


Figure 14. Residuals of the cake filtration model fitted to precoat filtration data in Figure 9 vs time.

apparent some behavior is missed at the beginning of the filtration. The fact that the residuals are negative during the first 600 s of the experiments, indicates that the model is missing a phenomenon during this time period which would increase the pressure drop. It is likely that this is due to the depth filtration of the smallest particles in the precoat layer²⁵ since it is most pronounced at the start of the experiment. Still, the general trend of this filtration is well captured by the model, but multiple particle filtration can probably not be considered simple cake filtration alone. Adding this depth filtration can simply be done in eq 3 by summing an additional resistance term of which the increase would decay to 0 after some time (when the behavior shifts to cake filtration only) or having the initial resistance R_0 vary with time as well instead of being a constant. This will however add an additional parameter that needs to be estimated, along with the difficulty of distinguishing between the contributions of concurrently occurring phenomena. Alternatively, the simple pressure drop model (eqs 3 and 4) we now employ can be substituted by a more extensive model intended for filter-aid filtration. An example of such a model was shown by Pergam et al.,²⁶ based on the work of Stamatakis and Tien.²⁴

CONCLUSIONS

In order to be able to get information on the whole filtration step in solid–liquid separation on equipment that is similar to that employed in industry, it is necessary to describe the transport in the filter vessel accurately. Here we have shown that the whole filtration behavior in a vertical filter vessel can be described by the residence time distribution of the vessel combined with the time it takes for particulates to travel along the length of the filter element. Using nonlinear parameter estimation allows for accurate estimation of both the specific cake resistance and delay caused by transport along the cloth without the need for linearization or arbitrary cropping of the data. Using only 2 points to measure the transport across the cloth and accounting for the geometry of the support, already a good approximation of this delay time can be estimated, with only a difference of 3 s (4% difference). A more accurate estimation could in the future eliminate the need to fit the delay time at all. In the case of filter-aid filtration, where we employ the filter-aid as a precoat layer, only considering cake filtration does not suffice anymore, and accounting for depth filtration is likely needed in the initial parts of the experiment. By analyzing the residuals of fitting the cake filtration-only

model, we can visually inspect when other phenomena are occurring.

■ ASSOCIATED CONTENT

SI Supporting Information

The Supporting Information is available free of charge at <https://pubs.acs.org/doi/10.1021/acs.iecr.4c04519>.

Detailed schematic of the experimental setup, photographs of the filter element, particle size distributions, regression analysis, and numerical investigations of delay time (PDF)

■ AUTHOR INFORMATION

Corresponding Authors

Jurgen B. Roman – *Soft Matter, Fluidics and Interfaces and Membrane Process Technology, University of Twente, Enschede 7500 AE, The Netherlands*; orcid.org/0000-0001-9964-8277; Email: j.b.roman@utwente.nl

Jeffery A. Wood – *Soft Matter, Fluidics and Interfaces, University of Twente, Enschede 7500 AE, The Netherlands*; orcid.org/0000-0002-9438-1048; Email: j.a.wood@utwente.nl

Authors

Antoine J.B. Kemperman – *Membrane Process Technology, University of Twente, Enschede 7500 AE, The Netherlands*; orcid.org/0000-0003-1763-212X

Walter G.J. van der Meer – *Membrane Process Technology, University of Twente, Enschede 7500 AE, The Netherlands*

Complete contact information is available at:

<https://pubs.acs.org/doi/10.1021/acs.iecr.4c04519>

Notes

The authors declare no competing financial interest.

■ ACKNOWLEDGMENTS

The authors thank Oasen NV for funding this work. The authors thank Amafilter for supplying a benchscale cricket filter and for fruitful discussion on the topic of cake filtration. The authors thank the JRS group for providing us with samples of cellulose fibers for usage in the project. The authors thank Frank Morssinkhof for help with assembling the experimental setup.

■ ADDITIONAL NOTE

¹Fitting exponents between 2 of the 4 stated values has little meaning, often ascribed to a combined behavior of the 2 closest values. It probably is more sensible to fit multiple values of k_1 with set values of k_2 , where the right side of eq 1 becomes a summation of these terms, as done for example by Mukai et al.¹³

■ REFERENCES

- (1) Tarleton, E.; Willmer, S. The Effects of Scale and Process Parameters in Cake Filtration. *Chem. Eng. Res. Des.* **1997**, *75*, 497–507.
- (2) Sparks, T.; Chase, G. In *Filters and Filtration Handbook*, 6th ed.; Welford, N., Ed.; Butterworth-Heinemann, 2013.
- (3) Tien, C. Cake filtration research—a personal view. *Powder Technol.* **2002**, *127*, 1–8.
- (4) Ruth, B. F.; Montillon, G. H.; Montonna, R. E. Studies in Filtration - I. Critical Analysis of Filtration Theory. *Industrial & Engineering Chemistry* **1933**, *25*, 76–82.
- (5) Ruth, B. F.; Montillon, G. H.; Montonna, R. E. Studies in Filtration - II. Fundamental Axiom of Constant-Pressure Filtration. *Industrial & Engineering Chemistry* **1933**, *25*, 153–161.
- (6) Ruth, B. F. Studies in Filtration III. Derivation of General Filtration Equations. *Industrial & Engineering Chemistry* **1935**, *27*, 708–723.
- (7) Ruth, B. F. Studies in Filtration IV Nature of Fluid Flow through filter septa and Its Importance in the Filtration Equation. *Industrial & Engineering Chemistry* **1935**, *27*, 806–816.
- (8) Alexandrov, S.; Odintsov, S. D.; Khuzhayorov, B. K.; Ibragimov, G.; Saydullaev, U.; Pansera, B. A. An Axi-Symmetric Problem of Suspensions Filtering with the Formation of a Cake Layer. *Symmetry* **2023**, *15*, 1209.
- (9) Hesse, R.; Lösch, P.; Antonyuk, S. CFD-DEM analysis of internal packing structure and pressure characteristics in compressible filter cakes using a novel elastic–plastic contact model. *Advanced Powder Technology* **2023**, *34*, No. 104062.
- (10) Sauer, F.; Henn, H.; Peuker, U.; Hoffner, B. Experimental Method Development for the Formation of Filter Cakes with Inhomogeneous Cake Geometry. *Chemie Ingenieur Technik* **2024**, *96*, 363–372.
- (11) Hermans, P. H.; Bredée, H. L. Zur Kenntnis der Filtrationsgesetze. *Recueil des Travaux Chimiques des Pays-Bas* **1935**, *54*, 680–700.
- (12) Tien, C.; Ramarao, B. V. Revisiting the laws of filtration: An assessment of their use in identifying particle retention mechanisms in filtration. *J. Membr. Sci.* **2011**, *383*, 17–25.
- (13) Mukai, Y.; Yue, Y.; Takiguchi, K. Dynamic behavior and mechanistic analysis in filtration of dilute particulate suspensions through nanofibrous membrane. *Colloids Surf., A* **2024**, *703*, No. 135270.
- (14) Schroeder, P. On the Advantages of Nonlinear Continuum Scale Filtration Models, Ph.D. thesis, Technische Universität München, 2023.
- (15) Todisco, S.; Peña, L.; Drioli, E.; Tallarico, P. Analysis of the fouling mechanism in microfiltration of orange juice. *Journal of Food Processing and Preservation* **1996**, *20*, 453–466.
- (16) Buchwald, T. Nonlinear Parameter Estimation of Experimental Cake Filtration Data, Ph.D. thesis, Technischen Universität Bergakademie Freiberg, 2021.
- (17) Tiller, F. M.; Li, W.; Alles, C. Dangers of lab-plant scaleup for filters involving solid/liquid systems. *Chem. Eng. Commun.* **2003**, *190*, 128–150.
- (18) FAN, K.; FU, W. Residence Time Distribution of Suspended Particle in Vertical Tubular Flow. *J. Food Sci.* **1996**, *61*, 982–985.
- (19) Palmieri, L.; Cacace, D.; Dipollina, G.; Dall'Aglio, G.; Masi, P. Residence time distribution of food suspensions containing large particles when flowing in tubular systems. *Journal of Food Engineering* **1992**, *17*, 225–239.
- (20) Hogendoorn, W.; Chandra, B.; Poelma, C. Onset of turbulence in particle-laden pipe flows. *Phys. Rev. Fluids* **2022**, *7*, No. L042301.
- (21) Benz, N.; Lösch, P.; Antonyuk, S. Influence of the Measurement Resolution on the Filtration Analysis: An Improved Test Setup According to VDI 2762 Guideline. *Processes* **2023**, *11*, 299.
- (22) Tiller, F. M.; Lu, W.-M. The role of porosity in filtration VIII: Cake nonuniformity in compression–permeability cells. *AIChE J.* **1972**, *18*, 569–572.
- (23) Fogler, H. S. *Essentials of Chemical Reaction Engineering*; Pearson PTG, 2017; Chapter 16.
- (24) Stamatakis, K.; Tien, C. Cake formation and growth in cake filtration. *Chem. Eng. Sci.* **1991**, *46*, 1917–1933.
- (25) Kuhn, M.; Briesen, H. Dynamic Modeling of Filter-Aid Filtration Including Surface- and Depth-Filtration Effects. *Chem. Eng. Technol.* **2016**, *39*, 425–434.
- (26) Pergam, P.; Kuhn, M.; Briesen, H. Optimal dosage strategies for filter aid filtration processes with compressible cakes. *Chem. Eng. Sci.* **2022**, *262*, No. 117989.